Surface-Induced Photoreduction of 4-Nitrobenzenethiol on Cu Revealed by Surface-Enhanced Raman Scattering Spectroscopy

Kuan Soo Shin,*,† Hyun Sook Lee,‡ Sang Woo Joo,† and Kwan Kim*,‡

Department of Chemistry, Soongsil University, Seoul 156-743, Korea, and Department of Chemistry, Seoul National University, Seoul 151-742, Korea

Received: April 20, 2007; In Final Form: June 20, 2007

A copper foil etched in a dilute solution of HNO_3 is free of carbon and oxygen, but the nanostructure formed thereby is highly active for surface-enhanced Raman scattering (SERS), especially when 632.8-nm radiation from a He/Ne laser is used as the excitation source. We found further that the copper foil thus prepared is also an efficient photoelectron emitter such that the SERS spectrum of 4-nitrobenzenethiol on copper is readily converted to that of 4-aminobenzenethiol under 632.8-nm radiation. This surface-induced photoreduction allowed us to prepare patterned binary monolayers on copper that showed different chemical reactivities. Using the binary monolayers as a lithographic template, we found that calcium carbonate could be grown selectively on the amine-group-terminated regions by adjusting the crystal growth conditions.

1. Introduction

Since the discovery of surface-enhanced Raman scattering (SERS), many theoretical and experimental studies on this effect have been performed.[1−4] Regarding the origin of SERS, it is generally accepted that two enhancement mechanisms, one a long-range electromagnetic effect and the other a short-range chemical effect, are simultaneously operative. The electromagnetic mechanism is based on the amplified electromagnetic field generated upon optical excitation of the surface plasmon resonance of nanoscale surface roughness features in the 10−100-nm range,[5−8] whereas the chemical enhancement mechanism is associated with the electronic coupling of molecules adsorbed on certain surface sites at atomic-scale roughness (such as atomic cluster, terraces, and steps) with the surface, leading to a situation similar to resonance Raman scattering.[9−11] Both mechanisms suggest the possibility of enhanced absorption and enhanced photochemistry for surface-adsorbed molecules.

Direct observation of a surface-enhanced photochemical reaction has indeed been reported.[12−27] Aromatic sulfides such as benzyl phenyl sulfide and dibenzyl sulfide adsorbed on silver undergo surface reactions involving facile cleavage of C−S bonds by 514.5-nm radiation.[17−21] As another example, 4-nitrobenzoic acid and 4-nitrobenzenethiol adsorbed on silver are converted under ambient conditions to 4-aminobenzoic acid and 4-aminobenzenethiol, respectively, upon irradiation by an argon ion laser (514.5 nm).[22−26] In most cases, it has been observed that the SERS peaks of the original nitro molecules gradually lose intensity and a new set of peaks appears. The new peaks rapidly increase in intensity as a function of the laser illumination time, suggesting that the nitro molecules are subjected to photoreaction on the silver surface. These molecules have been found, however, not to undergo such reactions on a gold surface with visible light. This indicates that Ag substrates can act as moderate photoelectron emitters.[21,27] In fact, the photoemission behavior of Ag is known to be different in many aspects from that of other metals.[28]

Using photochemical information gathered by SERS studies, we recently demonstrated that patterned binary organic monolayers can readily be formulated on silver substrates by surface-induced photoreactions.[23,29] Using the binary monolayers as a lithographic template, we further conducted site-specific chemical reactions including the selective growth of biominerals such as calcite on either the nitro-group-terminated regions or the amine-group-terminated regions by adjusting the crystal growth conditions. These visible-laser-induced surface reactions hardly took place for SAMs assembled on substrates other than Ag, however.[30]

Ever since the discovery of the SERS phenomenon, copper substrate has received much less attention than silver and gold owing to its inherent instability. Recently, SERS measurements for 4-aminobenzenethiol (4-ABT) assembled on powdered Cu substrates and the effect of Ag and Au nanoparticles on the SERS of 4-ABT on Cu powder have been reported.[31] Given the potential applications of copper as an inexpensive raw material in the development of various nano- and optoelectronic devices, it is desired to explore the characteristics of any possible surface-induced photoreaction occurring on nanostructured copper substrates. In this light, the SERS of 4-nitrobenzenethiol on copper was investigated in this work, and the conversion of 4-nitrobenzenethiol to 4-aminobenzenethiol by visible laser was found to occur more facilely on Cu than on Ag, indicating the remarkable photoelectron emitting characteristics of nanostructured copper.

To the best of our knowledge, this is the first report of surface-induced photoreduction of 4-nitrobenzenethiol adsorbed on Cu substrate revealed by SERS. Using this surface-induced photoreaction, we prepared patterned binary monolayers on copper with selectable surface chemical properties. Site-specific chemical reactions and patterned crystal nucleation were then performed with these monolayers. This novel surface group modification method will be very useful because fabrication of such patterned monolayers on engineered substrates is essential

* To whom correspondence should be addressed. E-mail: kshin@ssu.ac.kr (K.S.S.), kwankim@snu.ac.kr (K.K.). Tel.: +82-2-8200436 (K.S.S.), +82-2-8806651 (K.K.). Fax: +82-2-8244383 (K.S.S.), +82-2-8891568 (K.K.).

† Soongsil University.

‡ Seoul National University.

10.1021/jp073053c CCC: $37.00
Published on Web 10/03/2007

for the development of molecule-based optoelectronic and biomimetic devices and sensors.

2. Experimental Section

4-Aminobenzenethiol (4-ABT, 97%), 4-nitrobenznethiol (4-NBT, 80%), Au foil (0.1 mm thick), Ag foil (0.05 mm thick), Cu foil (0.05 mm thick), silver powder (2−3.5 μm, 99.9%), and copper powder (3 μm, dendritic, 99.7%) were purchased from Aldrich and used as received. Unless otherwise specified, other chemicals were reagent grade, and highly pure water with a resistivity of greater than 18.0 MΩ•cm (Millipore Milli-Q System) was used in the preparation of aqueous solutions.

The Au foil was made SERS-active by repeated oxidation−reduction treatments (25 times) from −0.28 V (held for 10 s) to 1.22 V (held for 5 s) at 500 mV/s in a deoxygenated 0.1 M aqueous KCl solution.[32] The gold sheet used as the working electrode was mechanically polished using a 0.05-μm alumina slurry before use, and all the potentials quoted in this work are versus that of a silver/silver chloride (Ag/AgCl) electrode. The Ag and Cu foils were made SERS-active by immersing them in diluted (1:1) HNO_3 solution for about 30−60 s. For the self-assembly of 4-NBT or 4-ABT on these substrates, the foils were immersed in 1 mM ethanolic solution of adsorbate for about 30 min.[33] For a comparative study, micrometer-sized Ag and Cu powders were also used as SERS-active substrates. For the self-assembly of 4-NBT on these powders, 0.05 g of Cu or Ag was placed in a small vial into which 10 mL of stock solution of 1 mM 4-NBT was subsequently added. After 1 h, the solution phase was decanted.

To make patterned organic monolayers on copper, SAMs of 4-NBT on a HNO_3-etched Cu foil were initially placed below the object lens on an *XY* stage (Newport M-462) equipped with a dc motor actuator (Newport 850F) that was controlled by a motion controller (Newport PMC200-P2). The sample surface was sequentially scanned in 10-μm steps, irradiated with an Ar^+ laser at the wavelength of 514.5 nm for 30 s. The crystallization of calcium carbonate was subsequently conducted by soaking the sample in a 10 mM $NaHCO_3$ aqueous solution (50 mL) for 20 min and then adding 10 mM $CaCl_2$ solution (50 mL). After the crystallization step (20 min), the substrate was rinsed with ethanol to remove any weakly bound $CaCO_3$ and then blown dry with N_2.

Raman spectra were obtained using a Renishaw Raman system model 2000 spectrometer equipped with an integral microscope (Olympus BH2-UMA). The 632.8-nm line from a 17-mW He/Ne laser (Spectra Physics model 127) or the 514.5-nm line from a 20-mW Ar^+ laser (Melles-Griot model 351MA520) was used as the excitation source. Raman scattering was detected over a 180° geometry with a Peltier-cooled (−70 °C) charge-coupled device (CCD) camera (400 × 600 pixels). The laser beam was focused on a spot approximately 1 μm in diameter with an objective microscope with a magnification on the order of 20×. The holographic grating (1800 grooves/mm) and the slit provided a spectral resolution of 1 cm^{-1}. The Raman band of a silicon wafer at 520 cm^{-1} was used to calibrate the spectrometer. Replicate measurements were made to verify that the spectra were a true representation of each experiment. Field-emission scanning electron microscope (FE-SEM) images were obtained with a JSM-6700F FE-SEM operated at 5.0 kV.

3. Results and Discussion

Figure 1a,b shows the normal Raman (NR) spectrum of neat 4-NBT and its SERS spectrum on a gold sheet taken using 632.8-nm radiation as the excitation source. The two spectra exhibit a decent correlation with each other. Although a few peaks related to the vibration modes involving sulfur are more or less shifted, the bands due to the benzene ring modes appear at nearly the same position. The complete absence of the S−H stretching peak in the SERS spectrum, observable at 2548 cm^{-1} for pure 4-NBT (not shown in these figures), indicates that 4-NBT is adsorbed on Au as thiolate after S−H bond cleavage. All of the peaks in Figure 1b can then be attributed to 4-nitrobenzenethiolate.[34] The prominent peak around 1340 cm^{-1} in both spectra can be assigned to the symmetric stretching vibration of the nitro group [$\nu_s(NO_2)$]. This indicates that surface-induced photoreduction did not take place for 4-NBT on Au. Figure 1c,d shows the SERS spectra of 4-NBT adsorbed on silver and copper foils, respectively, also obtained using 632.8-nm radiation as the excitation source. First, notice that a very distinct SERS spectrum is observed not only using an Ag foil but also using a Cu foil. Also notice that the SERS spectral patterns of 4-NBT on Ag and Cu foils are obviously different from that on the Au sheet. The appearance of several new peaks in the spectra in Figure 1c,d indicates that 4-NBT is subjected to photoreaction on Ag and Cu foils. As discussed later, the reaction product is presumed to be 4-ABT.

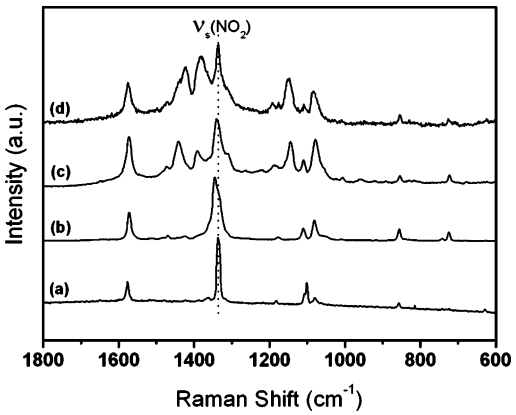

Figure 1. (a) Normal Raman spectrum of 4-NBT in the neat solid state. SERS spectra of 4-NBT adsorbed on (b) Au foil (electrochemically roughened), (c) Ag foil (etched using HNO_3), and (d) Cu foil (etched using HNO_3). All spectra were obtained using a He/Ne laser at 632.8 nm as the excitation source.

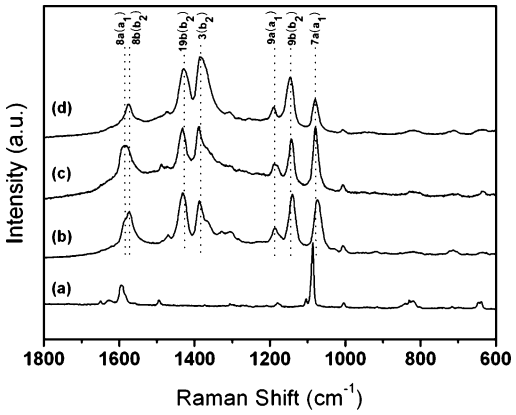

Figure 2. (a) Normal Raman spectrum of 4-ABT in the neat solid state. SERS spectra of 4-ABT adsorbed on (b) Au foil (electrochemically roughened), (c) Ag foil (etched using HNO_3), and (d) Cu foil (etched using HNO_3). All spectra were obtained using a He/Ne laser at 632.8 nm as the excitation source.

Figure 2a−d shows the NR spectrum of neat 4-ABT and its SERS spectra on Au, Ag, and Cu foils, respectively, obtained using 632.8-nm radiation as the excitation source. In the NR

TABLE 1: Raman Spectral Peak Assignments of 4-Aminobenzenethiol[a]

	SERS			
normal Raman	Au	Ag	Cu	assignment[b]
1594s	1591sh	1593s	1590sh	ν(CC), 8a(a_1)
1570sh	1574s	1579s	1575s	ν(CC), 8b(b_2)
1495w	–	–	–	ν(CC) + δ(CH), 19a(a_1)
–	1431vs	1432vs	1430vs	ν(CC) + δ(CH), 19b(b_2)
–	1388s	1389vs	1385vs	ν(CC) + δ(CH), 3(b_2)
1179w	1187m	1186m	1189m	ν(CH), 9a(a_1)
–	1140vs	1142vs	1145vs	ν(CH), 9b(b_2)
1087vs	1073vs	1077vs	1078s	ν(CS), 7a(a_1)
1005w	1006w	1007w	1007w	γ(CC) + γ(CCC), 18a(a_1)
829w	820vw	827vw	820vw	π(CH), 10a(a_2)
716vw	714w	713vw	711vw	π(CH) + π(CS) + π(CC), 4b(b_1)
642w	633vw	635w	635vw	γ(CCC), 12(a_1)

[a] vs, very strong; s, strong; m, medium; w, weak; vw, very weak; and sh, shoulder. [b] Assignments made by consulting refs 34 and 35, denoting ν, stretch; δ and γ, bend; and π, wagging. The ring modes correspond to those of benzene under C_{2v} symmetry.

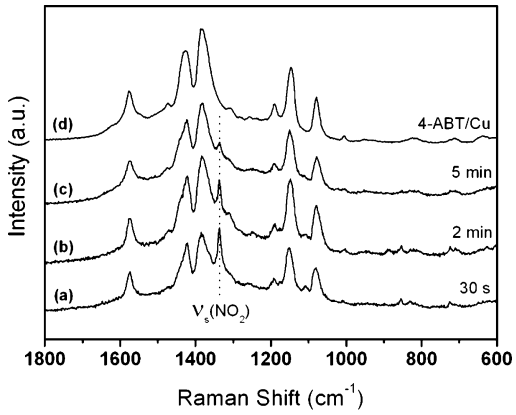

Figure 3. (a−c) Time-dependent SERS spectra of 4-NBT adsorbed on Cu foil (etched using HNO_3) recorded using a He/Ne laser at 632.8 nm as the excitation source. (d) SERS spectrum of 4-ABT adsorbed on Cu foil (etched using HNO_3) shown for comparison.

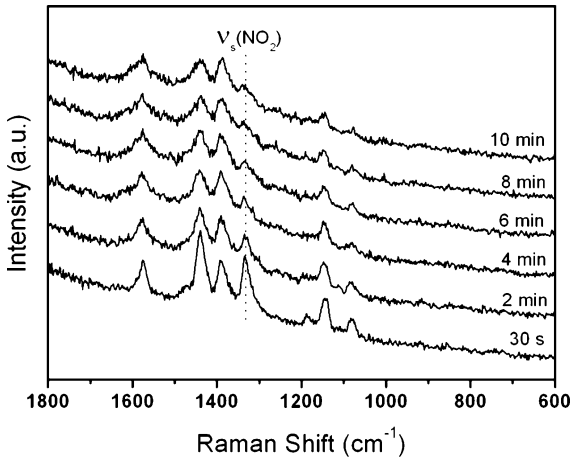

Figure 4. Time-dependent SERS spectra of 4-NBT adsorbed on Cu foil (etched using HNO_3) recorded using an Ar ion laser at 514.5 nm as the excitation source.

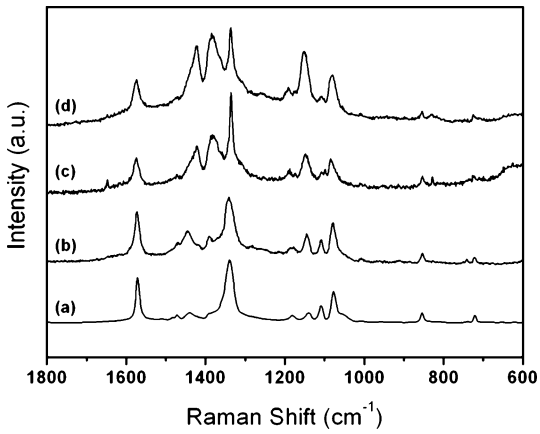

Figure 5. Substrate-dependent photoreduction of 4-NBT adsorbed on Ag and Cu substrates. SERS spectra of 4-NBT on (a) Ag powder (2−3.5 μm), (b) Ag foil (etched using HNO_3), (c) Cu powder (3 μm, dendritic), and (d) Cu foil (etched using HNO_3). All spectra were obtained using a He/Ne laser at 632.8 nm as the excitation source.

spectrum, the two strong peaks at 1087 and 1594 cm^{-1} can be assigned to the C−S and C−C stretching vibrations, respectively (a_1 vibration modes). In the SERS spectra, more enhanced peaks are observed around 1574, 1431, 1388, and 1140 cm^{-1}. Interestingly, these bands all belong to b_2-type modes,[35,36] as summarized in Table 1. Their apparent enhancement on silver has been ascribed in the literature to charge transfer (CT) from the metal to the adsorbed molecule.[36−38] In particular, the intensity of the peak at ∼1430 cm^{-1} varied as a function of the applied potential, in agreement with the CT mechanism, whereas the C−S stretching band at ∼1080 cm^{-1} was almost insensitive to the potential change because the band (a_1-type) was enhanced only via the EM mechanism. The similarities of the three SERS spectra in Figure 2 might then indicate that the CT mechanism is overwhelmingly operative not only on Ag but also on the Au and Cu substrates. The relative SERS enhancements of 4-ABT adsorbed on coinage metal substrates were evaluated from the SERS intensities shown in Figure 2b−d. In the case when a He/Ne laser (632.8 nm) was used as the excitation source, the relative enhancement factors for 7a band at ∼1080 cm^{-1} of 4-ABT on Au, Ag, or Cu substrates were estimated to be approximately 2.9:1.2:1.0. It seems difficult, however, to discuss the differences in substrate-dependent SERS enhancement in more detail because the Au substrate was electrochemically roughened whereas the Ag and Cu substrates were etched using HNO_3.

Figure 3 shows a series of SERS spectra of 4-NBT on a copper foil taken as a function of time under exposure to the 632.8-nm radiation from a He/Ne laser; the power at the sampling position was ∼1 mW. Figure 3a shows the SERS spectrum acquired within 30 s after exposure to the laser light. With increasing irradiation time, the $\nu_s(NO_2)$ peak at ∼1340 cm^{-1} gradually decreased, as shown in Figure 3b,c, and several new peaks emerged, for instance, at 1430, 1387, and 1144 cm^{-1}. For reference, the SERS spectrum of 4-ABT adsorbed on a Cu foil is reproduced in Figure 3d. It is evident that the new peaks in Figure 3b,c are caused by 4-ABT,

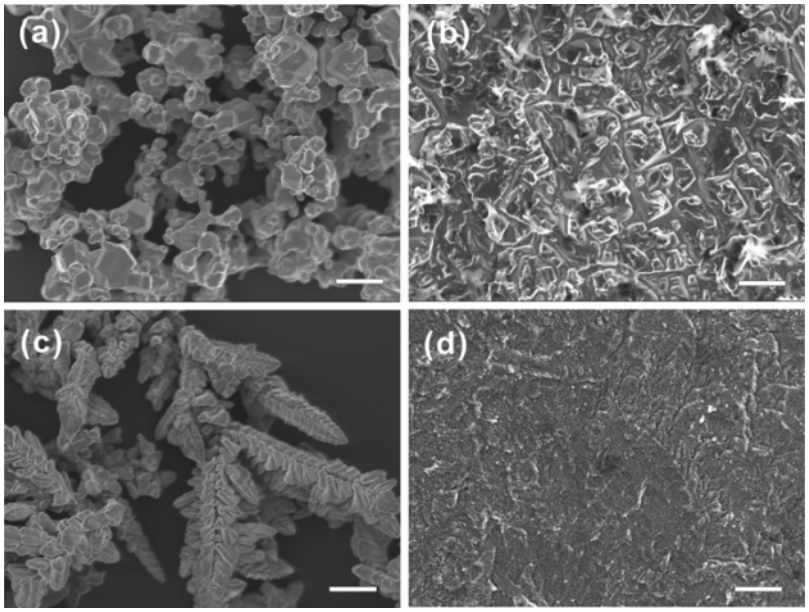

Figure 6. FE-SEM images of (a) Ag powder (2−3.5 μm), (b) Ag foil (etched using HNO_3), (c) Cu powder (3 μm, dendritic), and (d) Cu foil (etched using HNO_3).

indicating that 4-NBT on Cu is converted to 4-ABT upon exposure to 632.8-nm radiation. Because the reaction is reductive, electrons must be supplied from copper to 4-NBT. This implies that photoelectrons are generated from the copper substrate even by the irradiation of a visible laser.

To gain insight into the wavelength dependence of the surface-induced photoreaction, we also performed SERS measurements for 4-NBT on Cu foil using 514.5-nm radiation from an Ar^+ laser. Figure 4 shows a series of SERS spectra thus obtained as a function of laser irradiation time; the power at the sampling position was once again ~1 mW. The spectral changes observable using 514.5-nm radiation are much the same as those observed already for 632.8-nm excitation. It is intriguing that the conversion of 4-NBT to 4-ABT seems not to occur as rapidly under 514.5-nm radiation as it does 632.8-nm radiation. This is in sharp contrast to the usual understanding that a photoelectron is ejected more readily using a shorter- rather than a longer-wavelength laser. The present contradiction can be rationalized by assuming that the enhanced photoreaction at longer wavelength is deeply associated with the surface plasmon resonance of the nanostructured Cu substrates.

The characteristics of the photoreaction of 4-NBT to 4-ABT on Ag and Cu were found to be dependent on the substrate morphologies. Figure 5a,b shows the SERS spectra of 4-NBT adsorbed on Ag powder and Ag foil, respectively, measured using 632.8-nm radiation as the excitation source. The photoreaction of 4-NBT is seen to take place more readily on the surface of Ag foil than on Ag powder. Similarly, the photoreaction occurs more favorably on Cu foil than on powdered Cu, as can be seen in Figure 5d,c, respectively. The SERS spectrum of 4-NBT on Cu foil shown in Figure 3a is reproduced in Figure 5d. The different reaction kinetics must reflect the dissimilar electron emission efficiencies, which are, in turn, affected by the surface morphologies of the SERS-active nanostructures.[39] It is also apparent from Figure 5 that the photoconversion of 4-NBT to 4-ABT on copper is surprisingly faster than that on silver, when the He/Ne laser (632.8 nm) is used as the irradiation source.

The surface-induced photoreduction must involve charge transfer from the metal to the adsorbed molecule. The charge-transfer kinetics would then be affected by the energetics of the Fermi level of the metal substrate and/or the LUMO level of the adsorbate, which are subtly dependent on the morphology of the surface nanostructures. Regarding the surface nanostructures, certain degrees of surface roughness in the 10−100-nm range are known to be required for the electromagnetic enhancement mechanism to be operative for SERS, whereas atomic-scale roughness is necessary for the occurrence of chemical enhancement.[5−11] On these grounds, we recorded microscopy images of the silver and copper substrates. Figure 6a,b shows typical FE-SEM images of micrometer-sized silver powder and HNO_3-etched Ag foil, respectively. The surface of powdered silver appears to consist of a few tens of nanometer-

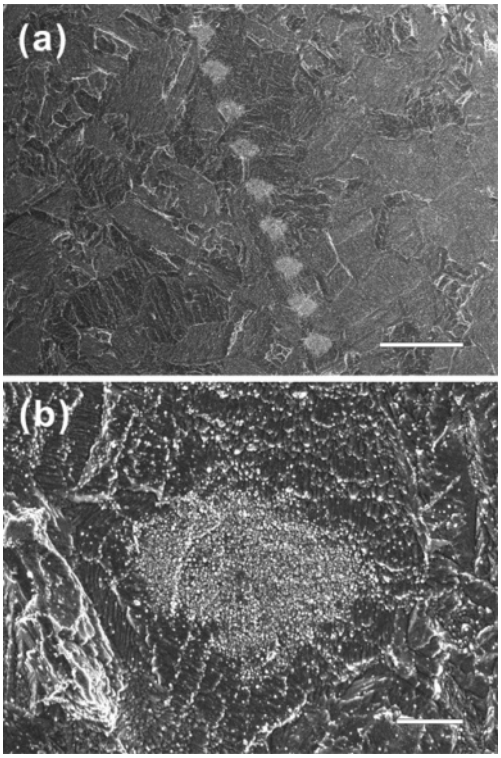

Figure 7. FE-SEM image of calcium carbonate crystals, at (a) lower and (b) higher magnification, formed on the amine-terminated regions that were generated previously using a focused 514.5-nm laser.

sized protrusions, whereas the surface of silver foil comprises domains around a few hundreds of nanometers in size. Figure 6c,d shows FE-SEM images of micrometer-sized dendritic copper powder and HNO_3-etched Cu foil, respectively. Although the differences in morphology cannot be quantified, the surfaces of all of the Ag and Cu substrates can be regarded as fractured nanoaggregates suitable for the occurrence of SERS and surface-induced photoreaction. Recall the earlier report that the surface roughening of silver not only causes a dramatic enhancement of the photoreaction yield at wavelengths close to the surface plasmon frequency but also leads to an extension of the photoresponse toward longer wavelengths.[40] A similar situation is thought to apply to Cu nanostructures. At least under 632.8-nm radiation, the photoelectrons generated from an etched Cu foil are more powerful than those from an Ag substrate for the conversion of 4-NBT to 4-ABT.

The production of patterned organic monolayers would then be possible through the photoinduced conversion of 4-NBT into 4-ABT on Cu surfaces. The formation of patterned, amine-terminated SAMs was, in fact, confirmed by the selective growth of calcium carbonate crystals. This is clear from the FE-SEM images shown in Figure 7a at lower magnification and in Figure 7b at higher magnification. For this crystallization, after self-assembly of 4-NBT on Cu, a focused Ar^+ ion laser (514.5 nm) was irradiated initially onto spots along a line separated from each other by 10 μm, and then calcium carbonate crystals were selectively grown on the substrate (see the Experimental Section). Crystallization was restricted to well-defined, amine-group-terminated regions and did not occur on the nitro-group-terminated regions. The crystallization of calcium carbonate only on the amine-group-terminated regions must be associated with the greater affinity of carbonate ions for amine groups rather than nitro groups. Once the calcium carbonate crystals nucleate at the amine-terminated sites, because of the mass-transport effect, the calcium and carbonate ions will be depleted over the nitro-terminated regions to a point of undersaturation so that crystallization hardly takes place in these regions. The present observation suggests, on one hand, that light-directed crystallization of calcium carbonate can be accomplished on a copper substrate at one's pleasure. The patterning method to form amine-group-terminated monolayers can be applied, on the other hand, for the fabrication of two-dimensional assemblies consisting of metal and semiconductor nanoparticles, fluorescent molecules, and biomolecules, etc.

4. Conclusion

Copper foil etched using dilute HNO_3 solution was found to be highly SERS-active when 632.8-nm radiation from a He/Ne laser was used as the excitation source. In addition, the copper foil appeared to be an efficient photoelectron emitter even under 632.8-nm radiation. The SERS spectrum of 4-nitrobenzenethiol on copper is thus readily converted to that of 4-aminobenzenethiol. On this basis, we demonstrated that patterned binary organic monolayers can readily be formulated on copper substrates by surface-induced photoreaction; such patterned binary organic monolayers can be used for the site-selective self-assembly of various nanoparticles including functional molecules. We definitely expect that both the higher SERS activity and the noticeable photoelectron emission characteristics of copper nanostructures are invaluable for the development of nano- and optoelectronic devices.

Acknowledgment. This work was supported by the Korea Science and Engineering Foundation (KOSEF R01-2006-000-10017-0). K.S.S. and S.W.J. were also supported by the Soongsil University Research Fund.

References and Notes

(1) Chang, R. K.; Furtak, T. E. *Surface Enhanced Raman Scattering*; Plenum Press: New York, 1982.
(2) Moskovits, M. *Rev. Mod. Phys.* **1985**, *57*, 783.
(3) Campion, A.; Kambhampati, P. *Chem. Soc. Rev.* **1998**, *27*, 241.
(4) Kneipp, K.; Kneipp, H.; Itzkan, I.; Dasari, R. R.; Feld, M. S. *J. Phys.: Condens. Matter* **2002**, *14*, R597.
(5) Moskovits, M. *J. Chem. Phys.* **1982**, *77*, 4408.
(6) Schatz, G. C. *Acc. Chem. Res.* **1984**, *17*, 370.
(7) Schatz, G. C.; Van Duyne, R. P. In *Handbook of Vibrational Spectroscopy*; Griffiths, P. R., Ed.; Wiley: New York, 2001; p 1.
(8) Moskovits, M.; Tay, L. L.; Yang, J.; Haslett, T. *Top. Appl. Phys.* **2002**, *82*, 215.
(9) Otto, A. In *Light Scattering in Solids*; Cardona, M., Guntherodt, G., Eds.; Springer-Verlag: Berlin, 1984; Vol. IV, p 289.
(10) Otto, A.; Mrozek, I.; Grabhorn, H.; Akemann, W. *J. Phys.: Condens. Matter* **1992**, *4*, 1143.
(11) Otto, A. *Phys. Status Solidi A* **2001**, *188*, 1455.
(12) Nitzan, A.; Brus, L. E. *J. Chem. Phys.* **1981**, *75*, 2205.
(13) Goncher, G. M.; Harris, C. B. *J. Chem. Phys.* **1982**, *77*, 3767.
(14) Goncher, G. M.; Parsons, C. A.; Harris, C. B. *J. Phys. Chem.* **1984**, *88*, 4200.
(15) Wolkow, R. A.; Moskovits, M. *J. Chem. Phys.* **1987**, *87*, 5858.
(16) Suh, J. S.; Jang, N. H.; Jeong, D. H.; Moskovits, M. *J. Phys. Chem.* **1996**, *100*, 805.
(17) Sandroff, C. J.; Herschbach, D. R. *J. Phys. Chem.* **1982**, *86*, 3277.
(18) Joo, T. H.; Yim, Y. H.; Kim, K.; Kim, M. S. *J. Phys. Chem.* **1989**, *93*, 1422.
(19) Yim, Y. H.; Kim, K.; Kim, M. S. *J. Phys. Chem.* **1990**, *94*, 2552.
(20) Lee, S. B.; Kim, K.; Kim, M. S. *J. Phys. Chem.* **1992**, *96*, 9940.
(21) Lee, I.; Han, S. W.; Kim, C. H.; Kim, T. G.; Joo, S. W.; Jang, D.-J.; Kim, K. *Langmuir* **2000**, *16*, 9963.
(22) Han, H. S.; Han, S. W.; Kim, C. H.; Kim, K. *Langmuir* **2000**, *16*, 1149.
(23) Han, S. W.; Lee, I.; Kim, K. *Langmuir* **2002**, *18*, 182.
(24) Kim, K.; Lee, I.; Lee, S. J. *Chem. Phys. Lett.* **2003**, *377*, 201.
(25) Lee, S. J.; Kim, K. *Chem. Phys. Lett.* **2003**, *378*, 122.
(26) Sun, S.; Birke, R. L.; Lombardi, J. R.; Leung, K. P.; Genack, A. Z. *J. Phys. Chem.* **1988**, *92*, 5965.
(27) Joo, S. W.; Han, S. W.; Kim, K. *Appl. Spectrosc.* **2000**, *54*, 378.
(28) Fedurco, M.; Shklover, V.; Augustynski, J. *J. Phys. Chem. B* **1997**, *101*, 5158.
(29) Han, S. W.; Lee, I.; Kim, K. *ETRI J.* **2004**, *26*, 38.
(30) Kim, K.; Lee, I. *Langmuir* **2004**, *20*, 7351.
(31) Kim, K.; Lee, H. S. *J. Phys. Chem. B* **2005**, *109*, 18929.
(32) Liu, Y. C. *Langmuir* **2002**, *18*, 174.
(33) Feng, Y.; Teo, W.-K.; Siow, K.-S.; Gao, Z.; Tan, K.; Hsieh, K. A.-K. *J. Electrochem. Soc.* **1997**, *144*, 55.
(34) Skadtchenko, B. O.; Aroca, A. *Spectrochim. Acta A* **2001**, *57*, 1009.
(35) Varsanyi, G. *Assignments for Vibrational Spectra of Seven Hundred Benzene Derivatives*; Wiley: New York, 1974.
(36) Osawa, M.; Matsuda, N.; Yoshii, K.; Uchida, I. *J. Phys. Chem.* **1994**, *98*, 12707.
(37) Zhu, Z.; Zhu, T.; Liu, Z. *Nanotechnology* **2004**, *15*, 357.
(38) Baia, M.; Toderas, F.; Baia, L.; Popp, J.; Astilean, S. *Chem. Phys. Lett.* **2006**, *422*, 127.
(39) Han, S. W.; Lee, K. Y. *Bull. Korean Chem. Soc.* **2005**, *26*, 1427.
(40) Kim, C.-W.; Villagrán, J. C.; Even, U.; Thompson, J. C. *J. Chem. Phys.* **1991**, *94*, 3974.